THE GEOLOGICAL SOCIETY OF AMERICA®

Nonequilibrium degassing, regassing, and vapor fluxing in magmatic feeder systems

J.M. Watkins[1]*, J.E. Gardner[2], K.S. Befus[3]
[1]Department of Earth Sciences, University of Oregon, 100 Cascade, 1275 E 13th Avenue, Eugene, Oregon 97405, USA
[2]Department of Geological Sciences, Jackson School of Geosciences, University of Texas at Austin, 2305 Speedway Stop C1160, Austin, Texas 78712, USA
[3]Department of Geosciences, Baylor University, Waco, Texas 76798, USA

ABSTRACT

Magma degassing models typically invoke volatile depletion of a single parental melt, with permeable loss of exsolved gas having served for many years as the paradigm for the transition from volatile-rich, explosive eruptions to volatile-depleted lava flows. These degassing models are guided by measurements of H_2O, CO_2, and hydrogen isotope variations retained in melt that quenched to glass, but the existing models are not uniquely constrained by the data. There also remains uncertainty surrounding the origin and significance of volcanic glass fragments. We show that individual obsidian pyroclasts from Mono Craters, California (USA), are heterogeneous in dissolved H_2O and CO_2, suggesting that clasts are assembled from juvenile melt and rewelded ash during magma ascent. This is in contrast to the conventional view that clasts are chemically homogeneous and sample the chilled, glassy margins of conduit walls. The new measurements of dissolved H_2O and CO_2 help reconcile existing open-system degassing models used to explain elevated CO_2/H_2O ratios, provide time scales based on diffusion modeling for pyroclast formation, and show that magma does not necessarily lose volatiles monotonically during ascent-driven decompression.

INTRODUCTION

The explosivity of volcanic eruptions depends on the abundance of volatile species, rate of volatile exsolution, and efficiency of gas removal from rising magma. These are difficult quantities to estimate because natural magmas are complex systems with chemical and physical properties that vary in both space and time. Much of what we know about the rates and efficiency of degassing is based on measurements of dissolved volatiles (H_2O and CO_2) and hydrogen isotopes in samples of volcanic glass (Castro et al., 2012, 2014; Taylor et al., 1983; Newman et al., 1988; Rust et al., 2004; Rust and Cashman, 2007).

Glassy obsidian clasts are volumetrically minor components of many tephra deposits, yet they provide important clues to magmatic degassing processes. Many of the ideas that underlie magmatic degassing models can be traced back to chemical analyses of dense, nearly bubble-free obsidian fragments from the A.D. 1340 eruption sequence at Mono Craters, California, USA (black circles in Fig. 1A; Taylor et al., 1983; Newman et al., 1988; Dobson et al., 1989; Rust et al., 2004; Barnes et al., 2014). A key observation is that CO_2/H_2O ratios are higher than what would be expected from simple closed- or open-system degassing of a single parental melt (solid curves in Fig. 1A; Newman et al., 1988). In closed-system degassing, bubbles are coupled to the melt and the melt composition adjusts to be in equilibrium with the total vapor exsolved. In open-system degassing, exsolved volatiles are removed from melt either by fast ascent of bubbles or through permeable pathways that allow vapor to escape. Note that the equilibrium curves are calculated from solubility relations, which do not provide information regarding the temporal evolution of vapor and melt compositions toward equilibrium (e.g., Newman and Lowenstern, 2002; Liu et al., 2005).

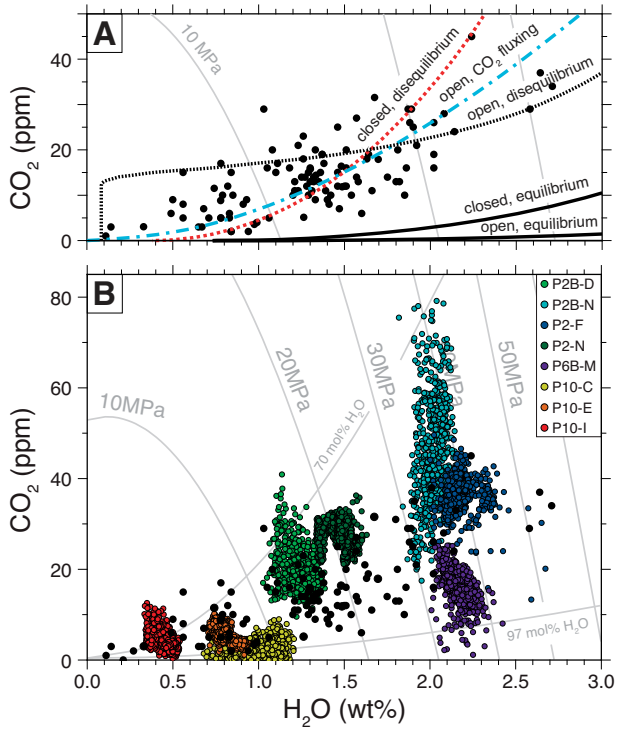

Figure 1. Measured concentrations of dissolved volatiles in obsidian pyroclasts from Mono Craters (California, USA). Black circles are spot analyses on pyroclasts from previous studies (Newman et al., 1988; Rust et al., 2004; Barnes et al., 2014). Gray curves are isobars and isopleths (curves of constant equilibrium vapor composition) assuming a magmatic temperature of 800 °C based on Fe-Ti oxide thermometry (Carmichael, 1966). A: Several different degassing models (dashed curves) have been proposed to explain the observation that CO_2/H_2O ratios are higher than expected from simple degassing of a single parental melt (solid black curves). B: Clasts are heterogeneous in dissolved CO_2 and H_2O.

Several different degassing models have been proposed to explain elevated CO_2/H_2O ratios, including open-system fluxing of a CO_2-rich vapor through previously degassed, brecciated magma (blue curve in Fig. 1A; Rust et al., 2004) or slow diffusion of CO_2 relative to H_2O in the melt toward vapor-filled fractures or bubbles during closed- or open-system degassing (red and black dotted curves in Fig. 1A; Gonnermann and Manga, 2005a). Although these models are not mutually exclusive (cf. Yoshimura and Nakamura, 2011), new types of measurements are needed to test the different degassing models and to guide future modeling developments.

*E-mail: watkins4@uoregon.edu

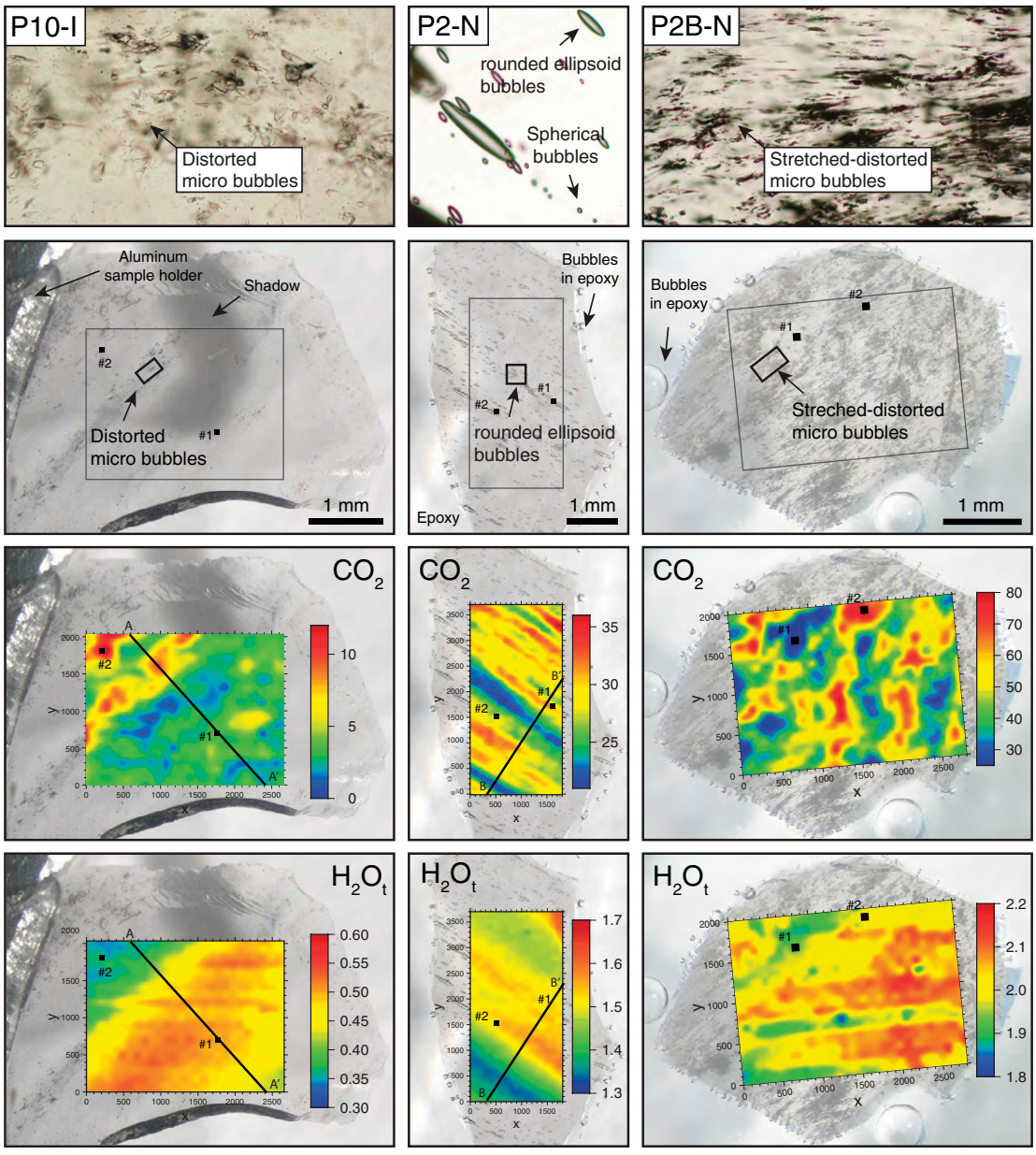

Figure 2. Distribution of dissolved CO_2 and H_2O in three representative pyroclasts that exhibit some of the key textures described herein. Left: P10-I has low volatiles but elevated CO_2 associated with two parallel bands of distorted microbubbles. Middle: P2-N has bands of elongated bubbles with a notable lack of correlation between bubble-rich bands and volatile concentrations. Right: P2B-N has the highest and most variable CO_2 of any clast. There is a clear correlation between elevated CO_2 and stretched-distorted bubbles. Transects for diffusion modeling (A-A′ and B-B′) are shown for P10-I and P2-N (see Fig. 3). Black squares show the locations of example Fourier transform infrared spectroscopy spectra in the Data Repository (see footnote 1). The vesicularities of these 3 samples are 0.16% (P10-I), 0.86% (P2-N), and 0.91% (P2B-N).

Many of the previous measurements are based on single (or a few) spot analyses of vesicle- and crystal-free regions of the clasts (Newman et al., 1988; Rust et al., 2004; Barnes et al., 2014). While this avoids complications that can be introduced by analyzing domains of a sample with different physical properties (see the GSA Data Repository[1]; von Aulock et al., 2014), it may be overlooking small-scale heterogeneities. We show that this is the case, and find that our results challenge the conventional view that obsidian pyroclasts are chemically homogeneous parcels of melt or glass, and are not fully consistent with any previously proposed degassing models.

GEOLOGICAL CONTEXT OF SAMPLES

The Mono Craters are a 17-km-long arcuate chain of rhyolite domes on the eastern flank of the central Sierra Nevada. The most recent eruptions spanned several years ca. A.D. 1340 and produced ~0.2 km^3 of pyroclastic fall, flow, and surge deposits, followed by extrusion of ~0.44 km^3 of lava flows and domes (Miller, 1985; Sieh and Bursik, 1986; Hildreth, 2004). The tephra section sampled for this study consists of soil at the base, overlain by 10 well-sorted lapilli layers that are rich in pumice clasts and less common obsidian clasts, interbedded with well-sorted ash-fall beds (Barnes et al., 2014). Pyroclastic obsidian clasts were collected from four of the coarser lapilli layers, including layers from near the base to near the top. We label the lapilli layers at each site stratigraphically (e.g., P2 comes from bed 2, early in the sequence), and those from Pit B include an additional indicator of B (e.g., P2B). Individual obsidian clasts are labeled with letters (e.g., P2B-A).

We selected eight obsidian clasts that collectively span the observed range of volatile contents (Barnes et al., 2014) and collected area maps of CO_2 and H_2O concentrations by Fourier transform infrared spectroscopy (see the Data Repository). We also made measurements of hydrous speciation (H_2O_m and OH, where m denotes molecular water), which yield cooling rates for six of the eight clasts that are consistent with glass formation by air quench as opposed to slow cooling in the subsurface (see the Data Repository).

VOLATILE HETEROGENEITY IN PYROCLASTS

The total range in volatile concentrations across the sample suite largely overlaps the range reported in previous studies based on spot

[1]GSA Data Repository item 2017049, details on sample information and processing, cooling rates, and diffusion modeing, is available online at www.geosociety.org/pubs/ft2017.htm, or on request from editing@geosociety.org.

analyses within clasts (Fig. 1B). An exception is clast P2B-N, which has higher and more variable CO_2 than any clast previously analyzed. There is a notable lack of positive correlation between H_2O and CO_2 within some clasts, and at least three of the samples (P6B-M, P10-E, and P10-I) exhibit negative correlations. Overall, the spread in volatile contents implies apparent equilibrium pressures of ~2.6–47 MPa and vapor compositions of ~70–97 mol% H_2O (Liu et al., 2005). The assumption of vapor-melt equilibrium, however, is not strictly valid, as evidenced by the preservation of large chemical gradients within clasts.

The relationships between volatile distributions and textures from three representative samples are particularly informative (Fig. 2). Area maps for the other five clasts are provided in Figures DR4 and DR5 in the Data Repository. The variations in CO_2 are of greater magnitude and shorter wavelength than variations in H_2O, probably as a consequence of the slower diffusion of CO_2 relative to H_2O (Zhang et al., 2007). In sample P10-I (left) and P2B-N (right), the elevated CO_2 contents correspond to regions of the clast containing distorted (P10-I) or stretched-distorted (P2B-N) bubbles in photomicrographs (top panels). In sample P10-I, the distorted bubbles separate a region of lower H_2O from a region of higher H_2O. This may represent a suture zone that now adjoins two parcels of melt that differ in dissolved H_2O contents. In sample P2B-N, the stretch-distorted bubbles are distributed throughout the clast. As discussed in the following, this may be the remnant of a CO_2-rich vapor in the interstices of incompletely sintering ash. A CO_2-rich magmatic vapor could be derived from the parent melt, from a different magma body deeper in the subsurface, or from calcined lake sediments in the wall rock (Rust et al., 2004; Rust and Cashman, 2007).

DIFFUSION MODELING

The preservation of volatile concentration gradients provides constraints on the amount of time that different parcels of melt within clasts have been in contact. We estimate this time scale using transects along the P10-I and P2-N area maps that lend themselves to one-dimensional diffusion modeling (A-A′ and B-B′ in Fig. 2). Details of the diffusion model are provided in the Data Repository. For rhyolite melt at 800 °C, the inferred diffusion time is 1 h to several hours (Fig. 3). As a general rule, the diffusion time (τ) scales with diffusion distance (L) as $\tau \sim L^2/D$, where D is the diffusivity of H_2O or CO_2. Because many of the other clasts exhibit shorter diffusion distances than the modeled transects (see the Data Repository), we conclude that the heterogeneities in H_2O and CO_2 were introduced to most clasts within tens of minutes to hours prior to the eruptive quench.

ORIGIN AND ASSEMBLY OF PYROCLASTS

The relatively short lived nature of millimeter-scale heterogeneities in dissolved CO_2 and H_2O requires processes capable of generating heterogeneities in volatile concentration at the submillimeter scale with sufficient frequency for them to be preserved in the erupted deposits. We conclude that these obsidian clasts are assembled from juvenile melt and hot ash as opposed to slowly cooled material excavated from eroded dikes, vanguard magma in wall-rock fractures, or welded fallback material from within the conduit (Newman et al., 1988; Rust and Cashman, 2007; McIntosh et al., 2014).

We envision a scenario whereby hot ash and gas ascend in the conduit and stick to the conduit walls. Initially, the interstitial gas between particles is trapped in the form of distorted vesicles that over time relax to a more spherical shape. The trapped gas may partially or completely resorb back into the melt, depending on temperature, pressure, and vapor composition (Fig. 1). At the same time, melt shearing promotes vesicle elongation, and if strain rates are high enough, the magma may shatter and be reincorporated back into the ascending mixture. Brittle deformation occurs when the shear stress exceeds the shear strength of the magma, which is <30 MPa for rhyolite at ~800 °C (Tuffen et al., 2003; Romano et al., 1996; Spieler et al., 2004). After stress release, shattered magma can

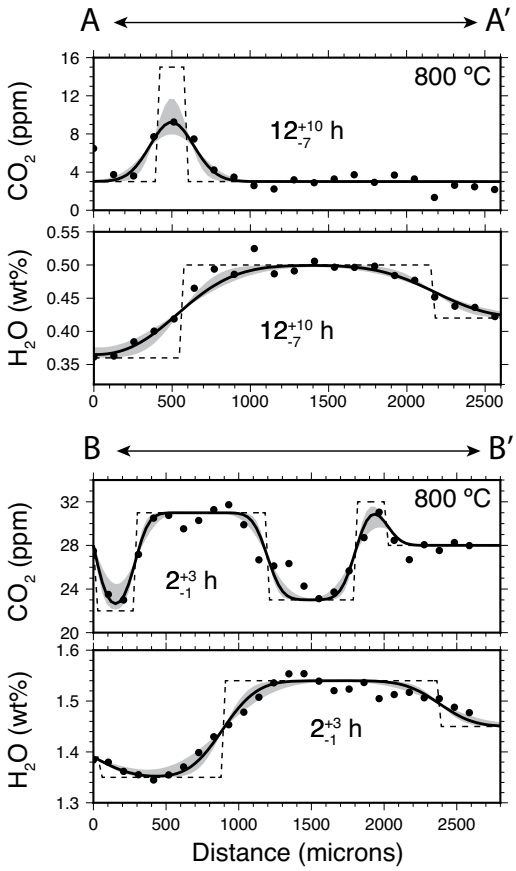

Figure 3. Gradients in H_2O and CO_2 are used to constrain the amount of time that different parcels of melt could have been in contact without homogenizing by diffusion. For the diffusion modeling, we assume a temperature of 800 °C and an appropriate pressure for each sample based on isobars (see Fig. 1B). The shaded areas show the range of diffusion profiles corresponding to the range of diffusion times quoted in the figure (superscripts and subscripts).

reweld and deform viscously, allowing stress to reaccumulate (Tuffen et al., 2003). Some of the shattered magma may survive as quenched obsidian clasts, whereas others may be destroyed by particle-particle collisions that lead to the production of ash and a repetition of this overall process. It is noteworthy that apparent equilibrium pressures do not vary by more than ~10 MPa for an individual clast (Fig. 1B), indicating that cycles of stress accumulation and relaxation to ~10 MPa may be superimposed on the overall decompression history.

IMPLICATIONS FOR DEGASSING MODELS

Most models of magma degassing assume that melt loses volatiles monotonically during ascent-driven decompression, but there are several ways in which this assumption may be oversimplified. First, vapor exsolved at depth may interact with shallow, relatively degassed melt, leading to volatile regassing (Rust et al., 2004; Yoshimura and Nakamura, 2010a). Second, as magma cools, bubbles may resorb and add volatiles back into the melt (Watkins et al., 2012; McIntosh et al., 2014). Third, it is possible for rising magma to undergo a complex stress history superimposed on the overall decompression path as a result of repeated shear fracturing and healing (Gonnermann and Manga, 2003, 2005b; Tuffen et al., 2003; Tuffen and Dingwell, 2005; Yoshimura and Nakamura, 2010b). This can lead to cycles of bubble growth and resorption on a time scale of hours (Watkins et al., 2012), or degassing and regassing through opening and closing of ash-filled cracks (Castro et al., 2012, 2014; Cabrera

et al., 2011). The nature of the small-scale heterogeneities described herein suggests that all of the processes listed may be contributing to the degassing-regassing history of Mono Craters magma.

The new data generally support the ideas that nonequilibrium degassing and/or fluxing of a CO_2-rich vapor contribute to the elevated CO_2/H_2O ratios (Fig. 1A; Rust et al., 2004; Gonnermann and Manga, 2005a). There are consequences of these models, however, that are inconsistent with the new data set. For example, the nonequilibrium degassing model posits that CO_2/H_2O ratios vary with bubble spacing. If bubble number densities (BND) are low (large spacing), then vapor-melt equilibration is slow and CO_2/H_2O ratios in the melt are high. The three samples in Figure 2 have very different BND, yet the one with the highest BND (P2B-N) has the highest CO_2/H_2O values. Our conceptual model, by contrast, produces high CO_2/H_2O in samples with higher BND by trapping heterogeneous gas between welding ash. This version of CO_2-fluxing differs notably from the model of Rust et al. (2004), who invoked vapor-melt equilibrium and continuous flushing of a CO_2-rich vapor through high-permeability fractures in magma along conduit walls. We argue that gas trapped between ash particles is more consistent with the small-scale, isolated heterogeneities we observe.

Although the obsidian pyroclast record of magma degassing may be more complicated than heretofore suspected, and challenges existing models for pyroclast generation, the nature of gradients in dissolved volatiles confirms that open-system processes are responsible for the production of vesicle-poor, degassed obsidian clasts (Rust et al., 2004; Gonnermann and Manga, 2005a). These types of measurements can be used to reevaluate magma degassing models at other localities and to probe time scales of active processes (e.g., ash sintering, magma deformation, and volatile resorption) in the subsurface that are generally inaccessible to direct observation.

ACKNOWLEDGMENTS

Figures were prepared using Generic Mapping Tools software (Wessel and Smith, 2013). This research was supported by National Science Foundation (NSF) grants EAR-1249404 to Watkins and EAR-1348050 to Gardner. Constructive reviews from Alison Rust, Kathy Cashman, and five anonymous reviewers strengthened the manuscript and supplemental information. We thank P. Wallace for access to laboratory facilities and for reviewing of an early version of this manuscript. Gardner thanks E. Llewllyn and the Institute for Advanced Studies, Durham University, for fruitful discussion and hospitality during preparation of this manuscript.

REFERENCES CITED

Barnes, J.D., Prather, T.J., Cisneros, M., Befus, K., Gardner, J.E., and Larson, T.E., 2014, Stable chlorine isotope behavior during volcanic degassing of H_2O and CO_2 at Mono Craters, CA: Bulletin of Volcanology, v. 76, p. 1–13, doi:10.1007/s00445-014-0805-y.

Cabrera, A., Weinberg, R.F., Wright, H.M., Zlotnik, S., and Cas, R.A., 2011, Melt fracturing and healing: A mechanism for degassing and origin of silicic obsidian: Geology, v. 39, p. 67–70, doi:10.1130/G31355.1.

Carmichael, I.S., 1966, The iron-titanium oxides of salic volcanic rocks and their associated ferro-magnesian silicates: Contributions to Mineralogy and Petrology, v. 14, p. 36–64, doi:10.1007/BF00370985.

Castro, J.M., Cordonnier, B., Tuffen, H., Tobin, M.J., Puskar, L., Martin, M.C., and Bechtel, H.A., 2012, The role of melt-fracture degassing in defusing explosive rhyolite eruptions at volcán Chaitén: Earth and Planetary Science Letters, v. 333, p. 63–69, doi:10.1016/j.epsl.2012.04.024.

Castro, J.M., Bindeman, I.N., Tuffen, H., and Schipper, C.I., 2014, Explosive origin of silicic lava: Textural and δD-H_2O evidence for pyroclastic degassing during rhyolite effusion: Earth and Planetary Science Letters, v. 405, p. 52–61, doi:10.1016/j.epsl.2014.08.012.

Dobson, P.F., Epstein, S., and Stolper, E.M., 1989, Hydrogen isotope fractionation between coexisting vapor and silicate glasses and melts at low pressure: Geochimica et Cosmochimica Acta, v. 53, p. 2723–2730, doi:10.1016/0016-7037(89)90143-9.

Gonnermann, H.M., and Manga, M., 2003, Explosive volcanism may not be an inevitable consequence of magma fragmentation: Nature, v. 426, p. 432–435, doi:10.1038/nature02138.

Gonnermann, H.M., and Manga, M., 2005a, Nonequilibrium magma degassing: Results from modeling of the ca. 1340 AD eruption of Mono Craters, California: Earth and Planetary Science Letters, v. 238, p. 1–16, doi:10.1016/j.epsl.2005.07.021.

Gonnermann, H.M., and Manga, M., 2005b, Flow banding in obsidian: A record of evolving textural heterogeneity during magma deformation: Earth and Planetary Science Letters, v. 236, p. 135–147, doi:10.1016/j.epsl.2005.04.031.

Hildreth, W., 2004, Volcanological perspectives on Long Valley, Mammoth Mountain, and Mono Craters: Several contiguous but discrete systems: Journal of Volcanology and Geothermal Research, v. 136, p. 169–198, doi:10.1016/j.jvolgeores.2004.05.019.

Liu, Y., Zhang, Y., and Behrens, H., 2005, Solubility of H_2O in rhyolitic melts at low pressures and a new empirical model for mixed H_2O-CO_2 solubility in rhyolitic melts: Journal of Volcanology and Geothermal Research, v. 143, p. 219–235, doi:10.1016/j.jvolgeores.2004.09.019.

McIntosh, I., Llewellin, E., Humphreys, M., Nichols, A., Burgisser, A., Schipper, C.I., and Larsen, J., 2014, Distribution of dissolved water in magmatic glass records growth and resorption of bubbles: Earth and Planetary Science Letters, v. 401, p. 1–11, doi:10.1016/j.epsl.2014.05.037.

Miller, C.D., 1985. Holocene eruptions at the Inyo volcanic chain, California: Implications for possible eruptions in Long Valley caldera: Geology, v. 13, p.14–17.

Newman, S., and Lowenstern, J.B., 2002, VolatileCalc: A silicate melt–H_2O–CO_2 solution model written in Visual Basic for Excel: Computers & Geosciences, v. 28, p. 597–604, doi:10.1016/S0098-3004(01)00081-4.

Newman, S., Epstein, S., and Stolper, E., 1988, Water, carbon dioxide, and hydrogen isotopes in glasses from the ca. 1340 AD eruption of the Mono Craters, California: Constraints on degassing phenomena and initial volatile content: Journal of Volcanology and Geothermal Research, v. 35, p. 75–96, doi:10.1016/0377-0273(88)90007-8.

Romano, C., Mungall, J., Sharp, T., and Dingwell, D.B., 1996, Tensile strengths of hydrous vesicular glasses: An experimental study: American Mineralogist, v. 81, p. 1148–1154, doi:10.2138/am-1996-9-1013.

Rust, A., and Cashman, K., 2007, Multiple origins of obsidian pyroclasts and implications for changes in the dynamics of the 1300 BP eruption of Newberry Volcano, USA: Bulletin of Volcanology, v. 69, p. 825–845, doi:10.1007/s00445-006-0111-4.

Rust, A., Cashman, K., and Wallace, P., 2004, Magma degassing buffered by vapor flow through brecciated conduit margins: Geology, v. 32, p. 349–352, doi:10.1130/G20388.2.

Sieh, K., and Bursik, M., 1986, Most recent eruption of the Mono Craters, eastern central California: Journal of Geophysical Research, v. 91, p. 12,539–12,571, doi:10.1029/JB091iB12p12539.

Spieler, O., Kennedy, B., Kueppers, U., Dingwell, D.B., Scheu, B., and Taddeucci, J., 2004, The fragmentation threshold of pyroclastic rocks: Earth and Planetary Science Letters, v. 226, p. 139–148, doi:10.1016/j.epsl.2004.07.016.

Taylor, B.E., Eichelberger, J., and Westrich, H., 1983, Hydrogen isotopic evidence of rhyolitic magma degassing during shallow intrusion and eruption: Nature, v. 306, p. 541–545, doi:10.1038/306541a0.

Tuffen, H., and Dingwell, D.B., 2005, Fault textures in volcanic conduits: Evidence for seismic trigger mechanisms during silicic eruptions: Bulletin of Volcanology, v. 67, p. 370–387, doi:10.1007/s00445-004-0383-5.

Tuffen, H., Dingwell, D.B., and Pinkerton, H., 2003, Repeated fracture and healing of silicic magma generate flow banding and earthquakes?: Geology, v. 31, p. 1089–1092, doi:10.1130/G19777.1.

von Aulock, F.W., et al., 2014, Advances in Fourier transform infrared spectroscopy of natural glasses: From sample preparation to data analysis: Lithos, v. 206, p. 52–64, doi:10.1016/j.lithos.2014.07.017.

Watkins, J.M., Manga, M., and DePaolo, D.J., 2012, Bubble geobarometry: A record of pressure changes, degassing, and regassing at Mono Craters: California Geology, v. 40, p. 699–702, doi:10.1130/G33027.1.

Wessel, P., and Smith, WH.F.., 2013, Generic mapping tools: Improved version released: Eos (Transactions, American Geophysical Union), v. 94, p. 409–410.

Yoshimura, S., and Nakamura, M., 2010a, Chemically driven growth and resorption of bubbles in a multivolatile magmatic system: Chemical Geology, v. 276, p. 18–28, doi:10.1016/j.chemgeo.2010.05.010.

Yoshimura, S., and Nakamura, M., 2010b, Fracture healing in a magma: An experimental approach and implications for volcanic seismicity and degassing: Journal of Geophysical Research, v. 115, B09209, doi:10.1029/2009JB000834.

Yoshimura, S., and Nakamura, M., 2011, Carbon dioxide transport in crustal magmatic systems: Earth and Planetary Science Letters, v. 307, p. 470–478, doi:10.1016/j.epsl.2011.05.039.

Zhang, Y., Xu, Z., Zhu, M., and Wang, H., 2007, Silicate melt properties and volcanic eruptions: Reviews of Geophysics, v. 45, RG4004, doi:10.1029/2006RG000216.

Manuscript received 20 August 2016
Revised manuscript received 10 November 2016
Manuscript accepted 14 November 2016

Printed in USA